Journal of Functional Foods 77 (2021) 104331

Contents lists available at ScienceDirect

Journal of Functional Foods

journal homepage: www.elsevier.com/locate/jff

The flavonoid morin alleviates nuclear deformation in aged cells by disrupting progerin-lamin A/C binding

Jinsook Ahn [a,1], Tae-Gyun Woo [b,1], So-mi Kang [b], Inseong Jo [a,c], Jae-Sung Woo [d], Bum-Joon Park [b,*], Nam-Chul Ha [a,*]

[a] Department of Agricultural Biotechnology, Center for Food Safety and Toxicology, Center for Food and Bioconvergence, and Research Institute for Agriculture and Life Sciences, Seoul National University, Seoul 08826, Republic of Korea
[b] Department of Molecular Biology, College of Natural Science, Pusan National University, Busan 46241, Republic of Korea
[c] Current address: KoBioLabs, Inc., Seoul 08826, Republic of Korea
[d] Department of Life Sciences, Korea University, Seoul 02841, Republic of Korea

ARTICLE INFO

Keywords:
Morin
Nuclear lamin A/C
Progerin
Hutchinson-Gilford progeria syndrome
Premature aging syndrome
Anti-aging

ABSTRACT

Nuclear lamin A/C plays an important role in maintaining the nuclear envelope structure. Hutchinson-Gilford progeria syndrome (HGPS) is a premature aging disease caused by a silent mutation in the lamin A/C gene, leading to the production of a C-terminally truncated protein (progerin). A deformed nuclear shape is a hallmark of HGPS cells, which observed in normal aged cells. A recent study has found that progerin can directly interact with lamin A/C, which leads to nuclear deformation. In this study, we identified natural compounds that can disrupt this progerin-mediated interaction. Similar to the synthetic compound JH4, morin disrupted this progerin-mediated interaction. Treatment with 20 μM morin ameliorated nuclear deformation by more than 50% in progerin-expressing cells. As morin is a naturally occurring substance with anti-oxidative activity, it may be developed as a functional food to improve the lifespan and health of both HGPS patients and normal aging individuals.

1. Introduction

Nuclear lamins play an essential role in maintaining the structural integrity of nuclear envelopes. Nuclear lamin proteins exist as dimers in solution and self-assemble into high-order filamentous structures via lateral and longitudinal interactions in the nuclear inner membrane (Ahn, Jo, Kang, Hong, Kim, Jeong, et al., 2019b; Lilina, Chernyatina, Guzenko, & Strelkov, 2020). Lamin filaments are further assembled into a three-dimensional meshwork, which undergoes continuous remodeling to cope with biomechanical stresses (Belaadi, Aureille, & Guilluy, 2016; Cho, Irianto, & Discher, 2017; Hoffman, Smith, Jensen, Yoshigi, Blankman, Ullman, et al., 2020). It is well known that lamin filaments are assembled and disassembled depending on the cell cycle, maintaining various cellular functions (Dechat, Shimi, Adam, Rusinol, Andres, Spielmann, et al., 2007; Nigg, 1992; Ward & Kirschner, 1990).

Several mutations in lamin genes result in human genetic disorders, including muscular dystrophy, lipodystrophy, and premature aging (Ahn, Jo, Kang, Hong, Kim, Jeong, et al., 2019a; Burke & Stewart, 2002; Butin-Israeli, Adam, Goldman, & Goldman, 2012; Capell & Collins, 2006; Ghosh & Zhou, 2014). Hutchinson-Gilford progeria syndrome (HGPS) is a rare autosomal dominant genetic disease with symptoms of premature aging, which is caused by a mutation within exon 11 or intron 11 of the *LMNA* gene encoding lamin A and C (lamin A/C) (Fong, Vickers, Farber, Choi, Yun, Hu, et al., 2009; Goldman, Shumaker, Erdos, Eriksson, Goldman, Gordon, et al., 2004; Pollex & Hegele, 2004; Yang, Bergo, Toth, Qiao, Hu, Sandoval, et al., 2005). This mutation results in the atypical splicing of mRNA that leads to the expression of a shorter lamin A, known as progerin, with truncation of the C-terminal 50 amino acids (De Sandre-Giovannoli, Bernard, Cau, Navarro, Amiel, Boccaccio, et al., 2003). Progerin accumulation in cells causes nuclear deformation, such as nuclear membrane blebs and a reduction in nucleoplasmic lamin A (Booth-Gauthier et al., 2013; McCord, Nazario-Toole, Zhang, Chines, Zhan, Erdos, et al., 2013; Shumaker, Dechat, Kohlmaier, Adam, Bozovsky, Erdos, et al., 2006).

A recent study has revealed that the truncated C-terminal region of progerin promotes an aberrant interaction with the Ig-like domain-

* Corresponding authors.
E-mail addresses: bjpark1229@pusan.ac.kr (B.-J. Park), hanc210@snu.ac.kr (N.-C. Ha).
[1] These authors contributed equally to this study.

https://doi.org/10.1016/j.jff.2020.104331
Received 23 September 2020; Received in revised form 7 December 2020; Accepted 7 December 2020
Available online 14 January 2021

containing region of the normal lamin A/C, leading to nuclear deformation (Lee, Jung, Yoon, Kang, Oh, Lee et al., 2016). The synthetic compound JH4 was found to ameliorate aging phenotypes in both HGPS cells and normal aging cells (Lee et al., 2016) (Cao, Blair, Faddah, Kieckhaefer, Olive, Erdos, et al., 2011). As the atypical splicing of the *LMNA* gene and nuclear deformation have also been detected in normal aging cells (Cao, Capell, Erdos, Djabali, & Collins, 2007; Scaffidi & Misteli, 2006), studies on HGPS are important for understanding the normal physiological aging process.

Here, we screened for natural compounds that can inhibit the abnormal interaction between lamin A/C and progerin. The natural compound morin was identified in this screening. Morin (3, 5, 7, 2′, 4′-pentahydroxyflavone) has been shown to exhibit anti-oxidative activity, and it can be isolated from mulberry figs and oriental medicinal herbs (Morris, Gage, & SH, 1951). In addition, morin has various physiological effects, including anti-oxidative and anti-cancer effects (Chung, Oliva, Dwabe, & Vadgama, 2016; Zhang, Zhang, Thakur, Wang, Wang, Hu, et al., 2018). In this study, we demonstrated the possibility of developing a new anti-aging functional food ingredient with the natural compound morin.

2. Results

2.1. Screening for inhibitors of progerin-lamin A binding in the natural compound library

Previously, the synthetic compound JH4 was screened by ELISA with an immobilized lamin A middle region covering residues 301–565 (LMNA-M) and truncated C-terminal 50 amino acid residues (progerin, corresponding to residues 566–606 and 657–664 in lamin A) (Lee et al., 2016). In this study, we performed a similar ELISA using a natural compound library consisting of 80 substances at 500 μM. To firmly immobilize the lamin protein onto a polystyrene ELISA plate, the photocatalytic crosslinking reaction was initiated using Tris(bipyridine) ruthenium(II) chloride, which is rapidly converted into ruthenium(VIII) oxide under 450 nm visible light in the presence of sodium persulfate (Alpers, Gallhof, Stark, & Brasholz, 2016; Fancy, Denison, Kim, Xie, Holdeman, Amini, et al., 2000; Lewandowska-Andralojc & Polyansky, 2013) (Fig. 1a). The screening identified 3-indolebutyric acid, gossypol, fisetin, morin, and piperine as candidate inhibitors (Fig. 1b and c). Among the potential inhibitors, we decided to further investigate the activity of the flavonoid morin in terms of its toxicity and cost (Gadelha, Fonseca, Oloris, Melo, & Soto-Blanco, 2014).

2.2. Inhibition of the interaction between the Ig-like domain of lamin A and progerin by morin

Based on the results of ELISA with immobilized LMNA-M and glutathione S-transferase (GST)-fused recombinant progerin, we estimated that morin inhibited the interaction of the two proteins by 50% at 200 μM (Fig. 2a). Isothermal titration calorimetry (ITC) was performed to quantify the binding affinity of LMNA-M with progerin or morin. Since we observed that LMNA-M was separated into three specific fragments during the purification process, we used a shorter fragment covering residues 406–552, referred to as the Ig-like domain in this study. In comparison with LMNA-M, the Ig-like domain exhibited a similar or higher affinity to progerin (Supplementary Fig. 1). ITC results showed that the binding affinity between lamin A and morin was approximately two-fold stronger than that between lamin A and progerin (Fig. 2b). These results indicated that progerin could interact with the Ig-like domain of lamin A and that morin could prevent this interaction by coupling with the Ig-like domain.

2.3. Amelioration of nuclear deformation in progerin-expressing cells by morin

To examine the efficacy of morin in preventing nuclear deformation caused by the interaction of lamin A and progerin, we compared the nuclear shapes of HEK293 cells expressing normal full-length lamin A and full-length progerin after treatment with morin. We used lamin A or

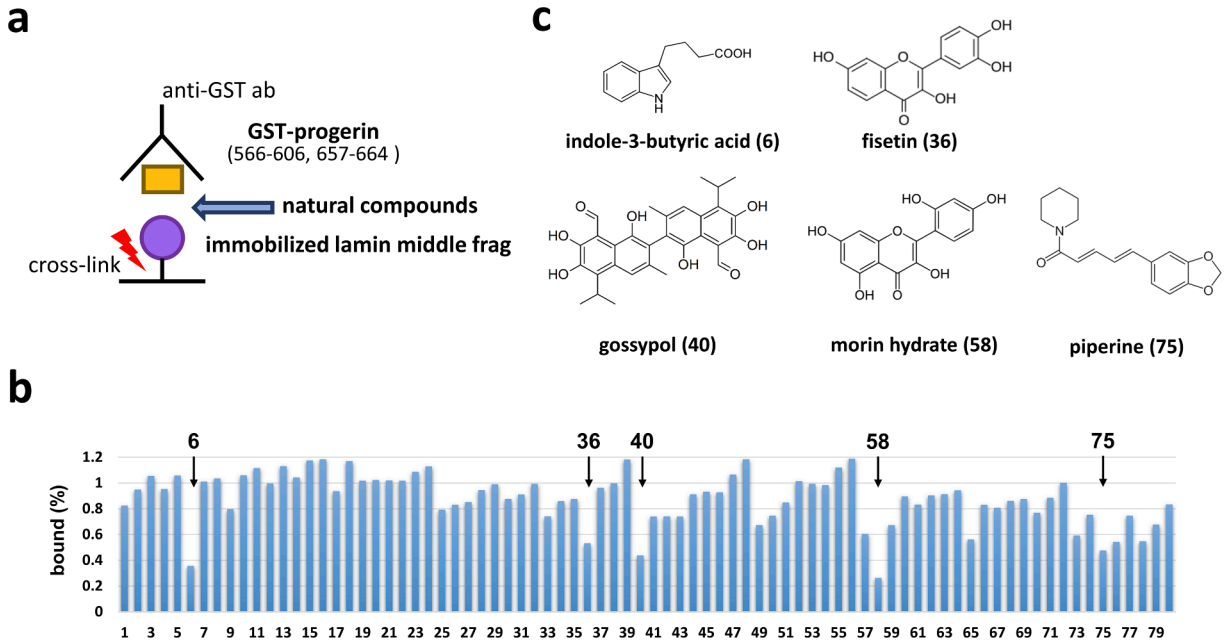

Fig. 1. Screening for inhibitors of progerin-lamin A binding. (a) Experimental scheme for natural compound screening. The purified lamin A middle region (301–565) was immobilized by photo-initiated protein crosslinking using Tris(bipyridine)ruthenium(II) chloride on the polypropylene plate. Each natural compound was added at 0.5 mM to each well. The GST-progerin C-terminal region (1 uM; residues 566–606 and 658–664) was also added to the wells. The binding of GST-progerin was detected by ELISA with anti-GST Ab. (b) Representative results of ELISA-based screening. The indicated bars were determined by a reaction carried out without the natural compounds. The arrows indicate hit compounds that inhibit the interaction of progerin with the lamin A middle region (301–565). (c) Molecular structures of selected natural compounds (6; indole-3-butyric acid, 36; fisetin, 40; gossypol, 58; morin hydrate).

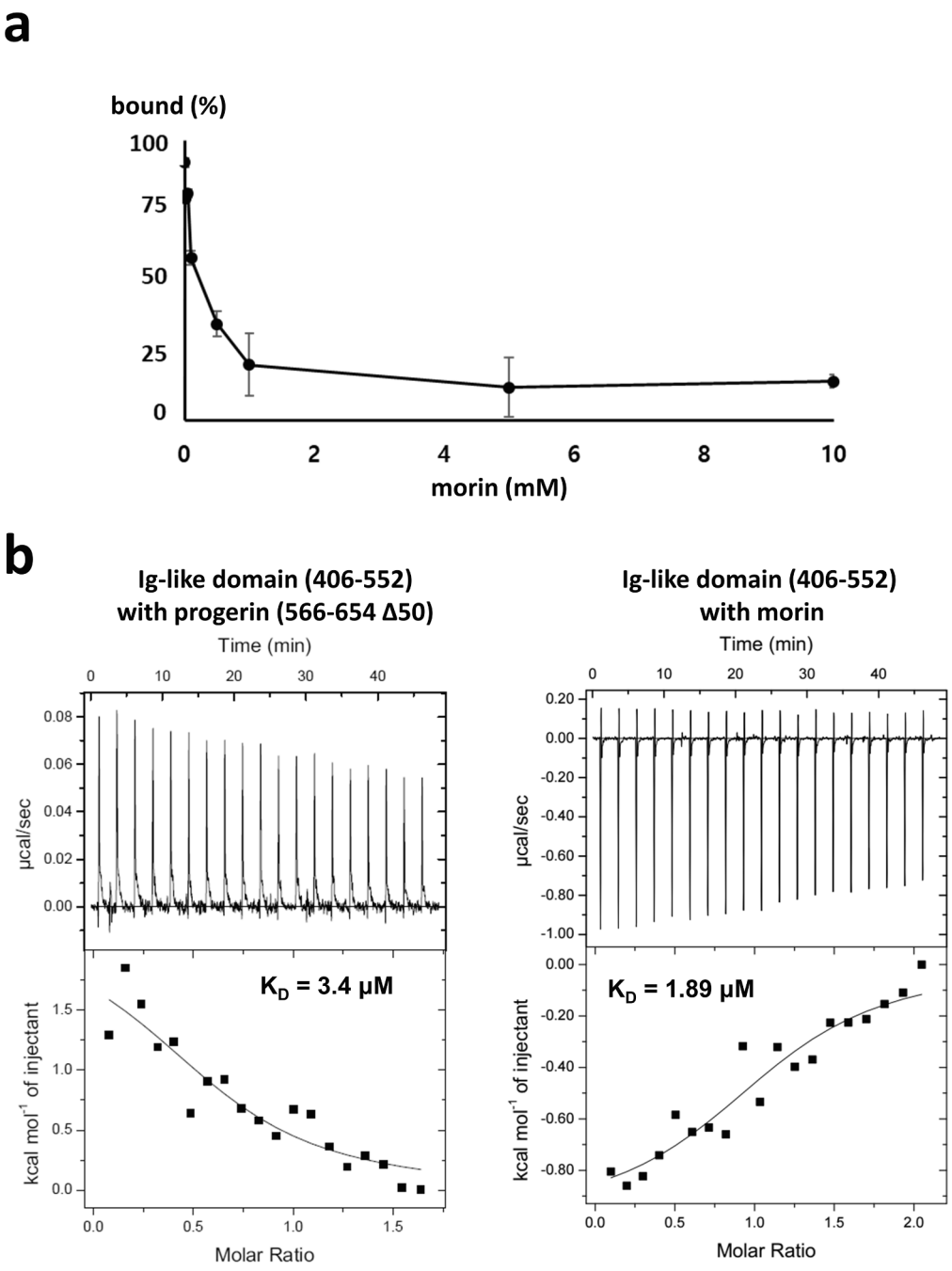

Fig. 2. Inhibition of the interaction between lamin A and progerin by morin via coupling with the Ig-like domain. (a) Dose-dependent relationship of the inhibition of the binding between lamin A and progerin by morin. Different concentrations of morin were used in the same ELISA. (b) ITC analysis of the binding of lamin A with progerin (*left*) or morin (*right*). The top panels represent the raw data plots as a series of peaks corresponding to the heat change (µcal/s) resulting from the titration of progerin or lamin (27 or 80 µM) with 19 injections of lamin or morin (180 or 500 µM; 2 µL per injection). The bottom panels show the integrated heat pulses in the top panels.

progerin constructs expressing GFP fusion proteins to visualize the cell envelope. In contrast to normal lamin A-expressing cells, progerin-expressing cells exhibited severe nuclear deformation (Fig. 3a). Morin markedly reduced nuclear deformation in progerin-expressing cells at 20 µM and showed a moderate effect at 10 µM (Fig. 3a). However, morin did not affect cells expressing lamin A (Fig. 3b).

To confirm the inhibitory role of morin, we performed GST pull-down assay of the GST-fused progerin C-terminal region and GFP-fused lamin A expressed in HEK293 cells. Cell lysates were incubated with resin-bound GST-progerin in the absence or presence of morin. Morin reduced the binding between progerin and lamin A in a dose-dependent manner (Supplementary Fig. 2).

2.4. Amelioration of nuclear deformation in HGPS cells by morin

We next examined the effect of morin on nuclear deformation in HGPS cells. We visualized the deformed nuclear envelopes of HGPS cells by immunofluorescence staining with lamin A antibody (Supplementary Fig. 3a). The treatment of HGPS cells with 10 µM morin for 3 days reduced the amount of nuclear deformation by 50% (Fig. 4a). Furthermore, the percentage of deformed nuclei was decreased to as low as 20% following treatment with 20 µM morin, and the treatment with 5 µM JH4 for the control showed a similar effect (Fig. 4a and Supplementary Fig. 3b). We also investigated the effect of morin on the senescence of HGPS cells. Decoy receptor 2 (DcR2) is a transmembrane receptor that is expressed in aged or senescent cells (Collado & Serrano, 2006). The transcriptional level of DcR2 was reduced by morin treatment; however, lamin A or progerin was not affected following treatment with morin

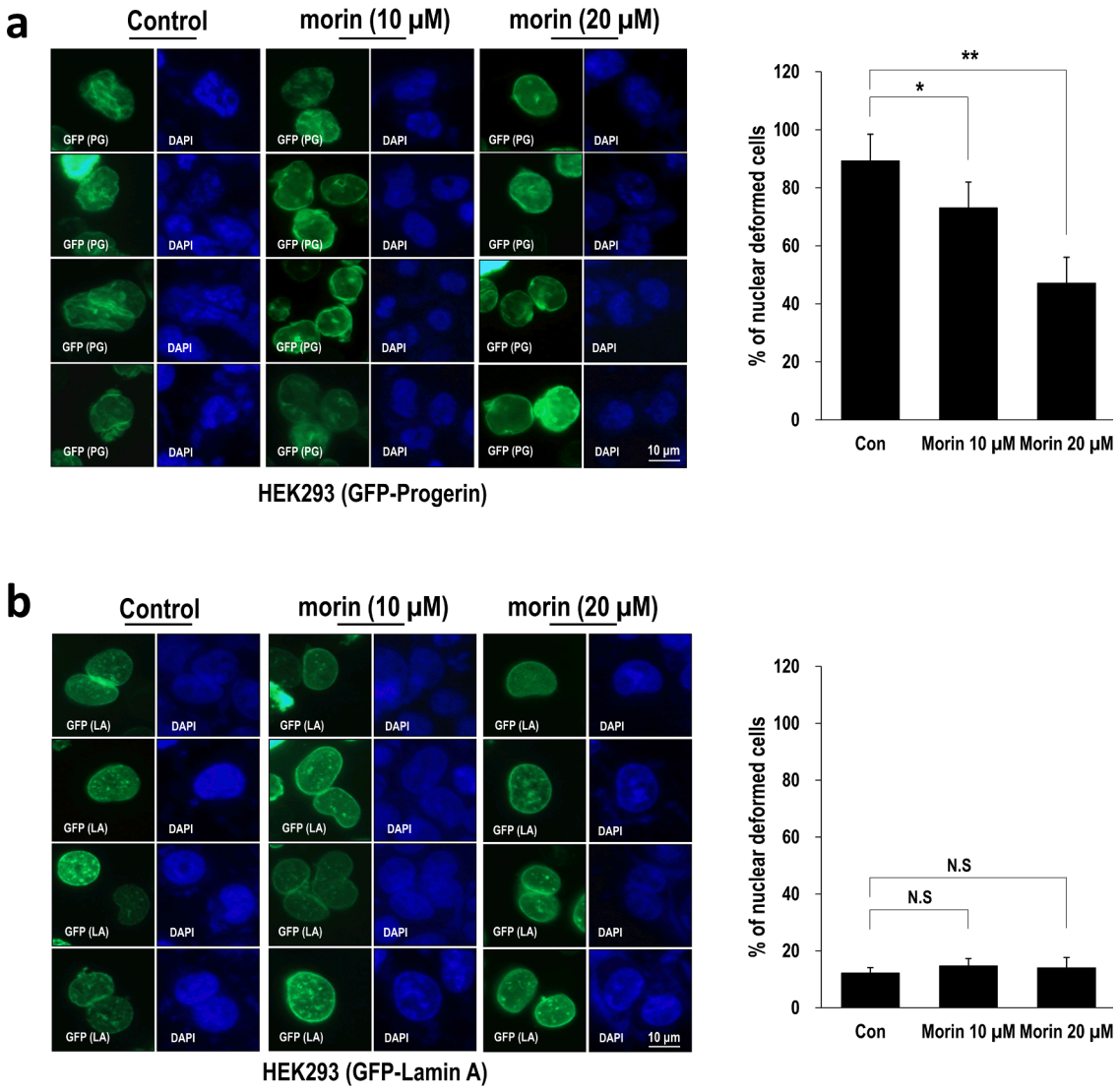

Fig. 3. Effect of morin on HEK293 cells expressing progerin. HEK293 cells were transfected with GFP-fused progerin (a, full-length, PG) or GFP-fused lamin A (b, full-length, LA). Treatment with morin was performed daily for 3 days at concentrations of 0, 10, and 20 μM. The nuclear envelope was visualized by the fluorescence of GFP fusion proteins (green), and the chromosomes were stained with DAPI (blue). Blebs, invaginations, and/or lobulations of the nuclear envelope were detected in GFP-PG-expressing cells but not in GFP-LA-expressing cells. The abnormality of the nuclear envelope was reduced with morin treatment in a dose-dependent manner. Nuclear envelope deformation was quantified based on the number of GFP-LA- or GFP-PG-expressing cells. *$P < 0.05$, **$P < 0.005$, N.S., not significant. (For interpretation of the references to colour in this figure legend, the reader is referred to the web version of this article.)

(Fig. 4b). These results suggest that morin may be used as a potential ingredient in functional foods to alleviate the symptoms of HGPS.

Nuclear deformation was observed in normal aging cells considering that progerin is generated during the normal aging process (J. S. Kim, Piao, Lee, Yoon, Moon, Lee, et al., 2013). We examined the effect of morin on cell proliferation using the senescence marker H3K9me3 (Hayflick, 1965). H3K9me3 is a heterochromatin marker that indicates trimethylation at the 9th lysine residue of histone H3 protein. In aged cells or HGPS cells, the level of H3K9me3 has been reported to be downregulated (Dechat, Pfleghaar, Sengupta, Shimi, Shumaker, Solimando, et al., 2008). We found a marginal increase in the expression of H3K9me3 in HGPS cells after treatment with 30 μM morin for 7 days (Fig. 5). When we treated HGPS cells with 20 μM morin for 5 days, nuclear deformation was ameliorated; however, there was no significant difference in H3K9me3 expression (Supplementary Fig. 4).

3. Discussion

In this study, we investigated morin as a direct inhibitor of progerin-mediated interactions using the purified Ig-like domain of lamin A/C and the C-terminal region of progerin. We evaluated the efficacy of morin in alleviating nuclear deformation in cells. Morin required a concentration four times higher than that of the synthetic compound JH4 to prevent nuclear deformation in HGPS cells. However, morin is advantageous as a daily food ingredient because of its potentially low toxicity; it is known to be harmless at around 300 mg/kg of body weight/day in mice (Wu, Zeng, Wu, & Fung, 1994; Yugarani, Tan, Teh, & Das, 1992).

In our previous study, we demonstrated that morin directly inhibited the activity of GSK3β, using biochemical and complex crystal structures (Gong, Park, Kim, Piao, Lee, Jo, et al., 2011; K. Kim et al., 2018). As the inhibition of GSK3β has been implicated in anti-inflammatory responses and the reduction of tau phosphorylation, morin has been suggested as a candidate agent for both anti-inflammatory activity and alleviation of Alzheimer's disease (Gong et al., 2011; Hooper, Killick, & Lovestone, 2008; Hur & Zhou, 2010; Piao, Lee, Kim, Yum, Stamos, Xu, et al., 2008). In this study, we discovered another effect of morin by chance in independent screening trials. It may be important to enhance the biomass of

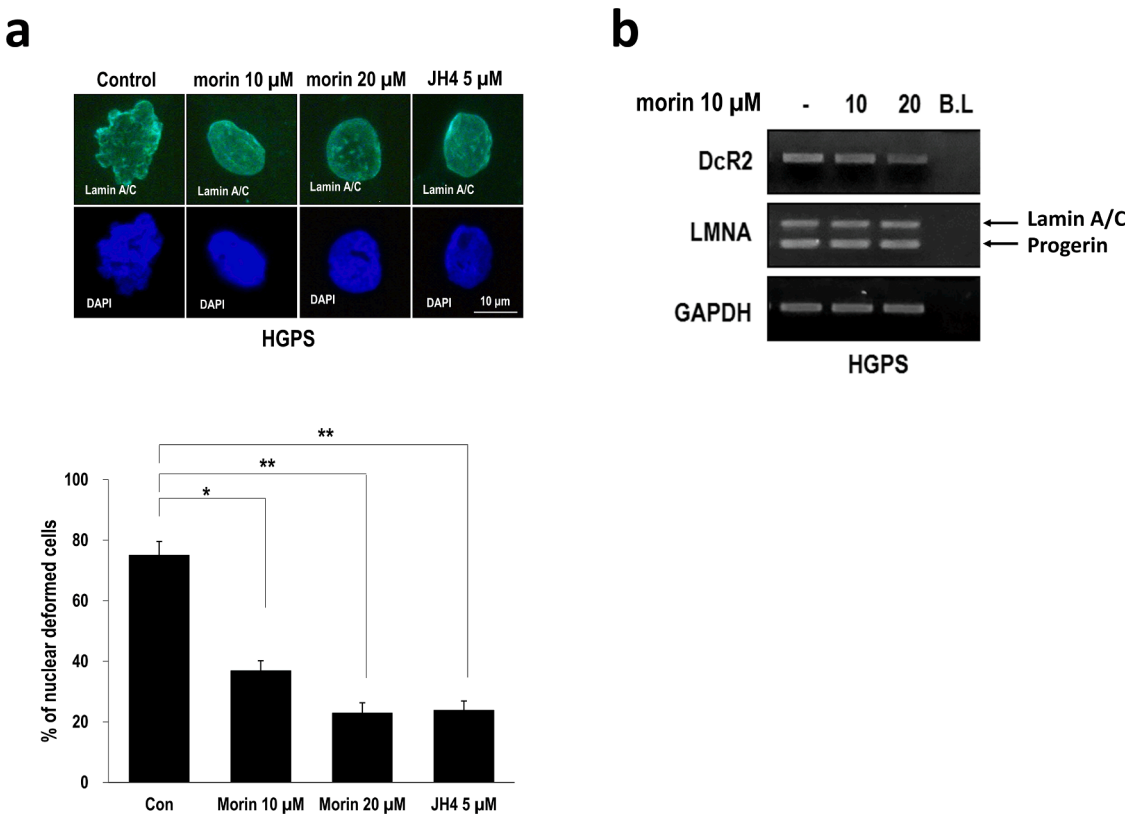

Fig. 4. Effect of morin on HGPS cells. (a) Fibroblast cells from HGPS patients were treated with morin (10 or 20 μM) or JH4 (5 μM). The nuclear envelope was visualized by immunofluorescence staining using anti-lamin A/C (green). The chromosomes were stained with DAPI (blue). The lower percentage of cells with deformed nuclear morphology in the images indicated that morin ameliorated nuclear deformation in HGPS cells (*bottom*). *$P < 0.05$, **$P < 0.005$. (b) Transcriptional levels of lamin A, progerin, and DcR2 in morin-treated HGPS cells. DcR2 expression was inhibited by morin (20 μM) treatment for 3 days. Lamin A and progerin expression was not altered by morin treatment at the RNA level. After HGPS cells were incubated with morin for 3 days, the total RNA was extracted, and RT-PCR was performed. (For interpretation of the references to colour in this figure legend, the reader is referred to the web version of this article.)

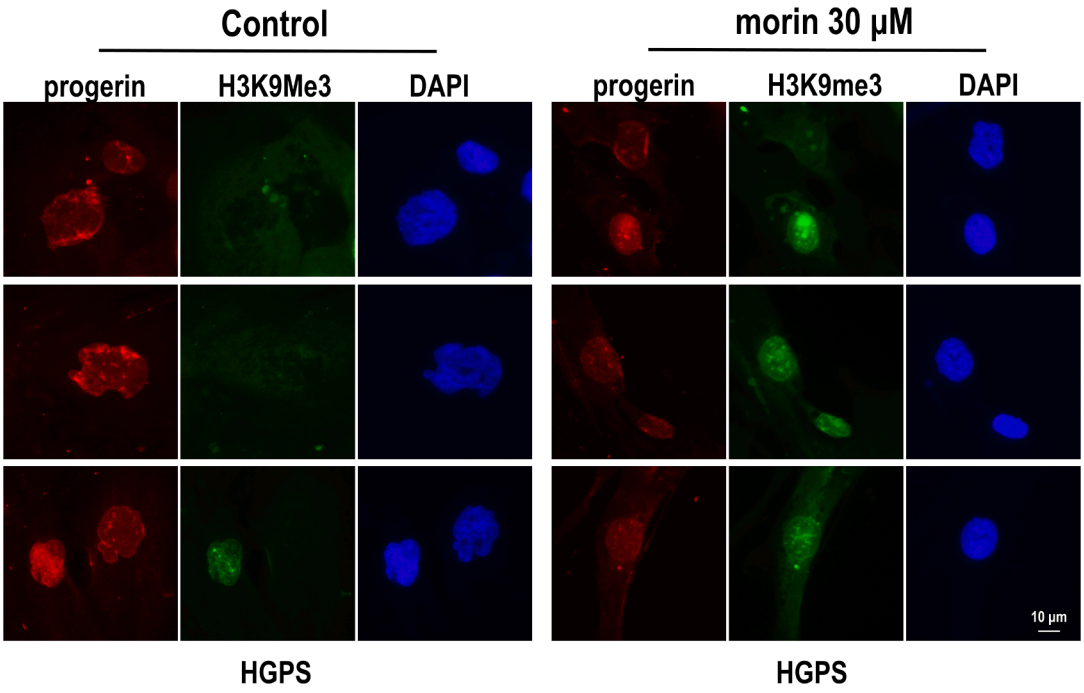

Fig. 5. Expression of H3K9me3 in HGPS cells after treatment with morin for 7 days. HGPS cells were incubated with morin (30 μM) for 7 days, and the senescence marker H3K9me3 was monitored. The deformation of the nuclear envelope was ameliorated with morin treatment; however, H3K9me3 expression was marginally increased. After fixation with 4% paraformaldehyde, the cells were stained with anti-progerin (red) and anti-H3K9me3 (green). Nuclei were stained with DAPI (blue). (For interpretation of the references to colour in this figure legend, the reader is referred to the web version of this article.)

morin in nature as the functional utility of morin increases (T. Khan, Abbasi, & Khan, 2018; Tariq Khan, Abbasi, Khan, Azeem, & products, 2017; Taimoor Khan, Khan, Hano, Abbasi, & Products, 2019).

Morin and quercetin are plant flavonols, which are secondary metabolites from polyphenolic flavonoid groups sharing a 3-hydroxyflavone backbone (Chen, Chan, Ho, Fung, & Wang, 1996; Rice-Evans, Miller, & Paganga, 1996). Quercetin is a well-known and powerful antioxidant among the flavonoids, and it has a higher electron donor ability compared with that of morin (Duenas, Gonzalez-Manzano, Gonzalez-Paramas, & Santos-Buelga, 2010; Rice-Evans et al., 1996). However, quercetin did not significantly reduce the progerin-mediated interaction in this study despite its higher anti-oxidative activity. Therefore, our findings suggest that morin's anti-oxidative activity is unlikely to be involved in the inhibition of the interaction between progerin and lamin.

Lamin should be continuously disassembled and reassembled in the remodeling process to cope with external mechanical stresses on the nucleus (Belaadi et al., 2016; Cho et al., 2017; Hoffman et al., 2020). Moreover, the lamin meshwork should be completely disassembled during mitosis, which is important for reforming the normal lamin meshwork after cell division (Dechat et al., 2007; Nigg, 1992; Ward & Kirschner, 1990). We believe that the abnormal and additional interactions mediated by progerin would hinder the disassembly of lamin filaments during the remodeling process. The results demonstrated that morin could interfere with the binding between the Ig-like domain and the C-terminal region of progerin. To gain more insight into the inhibitory mechanism of morin, we are currently attempting to determine the complex structure of the Ig-like domain and morin.

Morin has been proposed as an inhibitor of GSK3β to alleviate inflammation and tau phosphorylation. In this study, we showed another function of morin in the amelioration of premature aging. As a functional nutritional supplement, morin could contribute to the development of novel methods to treat a wide range of diseases related to normal aging.

4. Materials and methods

4.1. Cell culture

Human fibroblast cells from HGPS patients (AG03198) were obtained from Coriell Cell Repositories (Camden, NJ, USA), and HEK293 cells were purchased from the Korean Cell Line Bank (KCLB; Seoul, South Korea). HGPS cell lines were maintained in minimum essential medium (MEM) containing 15% fetal bovine serum, 2 mM glutamine, and 25 mM HEPES without antibiotics. HEK293 cells were cultured in MEM containing 10% fetal bovine serum, 25 mM HEPES, and 1% penicillin–streptomycin at 37 °C with 5% CO_2.

4.2. Plasmid construction and purification

To investigate protein–protein interactions, recombinant proteins were generated. A recombinant lamin A middle region (residues 301–564) and GST-fused recombinant progerin C-terminal region (GST-progerin, corresponding to residues 566–606 and 657–664 in lamin A) were used (Lee et al., 2016). The amplified DNA fragment encoding human lamin A (406–552) with the hexahistidine tag was inserted into the pPro-Ex-HTa vector (Thermo Fisher Scientific, Waltham, MA, USA). The plasmids were transformed into the *E. coli* BL21 (DE3) strain.

4.3. Purification of recombinant proteins

The transformed cells were cultured in 2 L of Terrific Broth medium containing 100 μg/mL ampicillin and 34 μg/mL chloramphenicol at 37 °C until an OD600 of 1.0 was reached. Then, the expression of proteins was induced using 0.5 mM IPTG at 30 °C for 6 h. After the cells were harvested by centrifugation, the cells were resuspended in lysis buffer containing 20 mM Tris-HCl (pH 8.0), 150 mM NaCl, and 2 mM 2-mercaptoethanol. The cells were disrupted using a continuous-type French press (Constant Systems Limited, Daventry, UK) at 23 kpsi. After centrifugation at 19,000*g* for 30 min at 4 °C, the cell debris was removed. The supernatant was loaded onto a TALON cobalt-based affinity resin (GE Healthcare, USA). The target proteins tagged with hexahistidine were eluted with lysis buffer supplemented with 250 mM imidazole and 0.5 mM ethylenediaminetetraacetic acid (EDTA). GST-fused recombinant progerin was purified using a GSH-agarose resin. Then, the target proteins were loaded onto a HiTrap Q column (GE Healthcare, USA). A linear gradient of increasing NaCl concentration was applied to the HiTrap Q column. The purified protein was concentrated and stored at −80 °C until use for further biochemical assays.

4.4. Modified ELISA

To isolate inhibitors of progerin-lamin A binding from a library of natural compounds (L1400; Selleckchem, Houston, TX, USA), an ELISA was established by modifying a previously described platform (Lee et al., 2016). His-LMNA-M was fixed on 96-well plates using 2 mM Tris (bipyridine)ruthenium(II) chloride with 10 mM sodium persulfate. After blocking and washing, the natural compounds (500 μM) were added to the plates. The 96-well plates were then washed with TBST (TBS + Tween20) and incubated with progerin. Next, we added anti-GST antibody (Ab; 1:1,000, 2 h) and anti-mouse-IgG-HRP (1:50,000, 1 h) sequentially. After washing twice, the plates were incubated with TMB solution (CL07; Calbiochem) and stop solution (1 N H_2SO_4), and the absorbance at 450 nm was determined.

4.5. Inhibition assay

Reactions were performed under the conditions described for chemical screening. Morin was diluted in 10% DMSO at concentrations ranging from 0.001 to 10 mM. Next, 10 μM His-LMNA-M was coated and fixed on 96-well plates. After incubation with the GST-progerin C-terminal region and morin at different concentrations for 1 h, anti-GST Ab (1:1000, 2 h) and anti-mouse-IgG-HRP (1:50,000, 1 h) were added to the plates. After washing, the plates were incubated with TMB solution (CL07; Calbiochem) and stop solution (1 N H_2SO_4) sequentially. The absorbance of the plates was read at 450 nm.

4.6. ITCxxx

ITC experiments were performed using an Auto-iTC200 microcalorimeter (GE Healthcare) at the Korea Basic Science Institute (Ochang, Korea). GST-fused progerin (370 μL; 27 μM) was prepared, and the His-tagged Ig-like domain (180 μL; 178 μM) was loaded into an injectable syringe. To determine the binding affinity between the Ig-like domain and morin, we prepared the samples at 80 μM and 500 μM, respectively. All samples were dialyzed overnight with PBS. A total of 19 injections (2 μL) were performed at 25 °C at intervals of 150 s while the titration syringe was stirred at 750 rpm. The data were analyzed using MicroCal Origin™ software.

4.7. Transfection system

GFP-fused lamin A (GFP-LA) and GFP-fused progerin (GFP-PG) expression vectors were provided by Misteli T (National Cancer Institute). Transfection was performed using Jet-PEI reagent (jetPEI; Polyplus-transfection, New York, NY, USA) according to the manufacturer's protocol. In brief, the vector (1.5 μg) was mixed with 1.5 μL of jetPEI reagent in 150 mM NaCl solution. The mixture was incubated for 15 min at room temperature. Subsequently, the mixture was added to the cells and incubated for 24–48 h.

4.8. GST pull-down assay and immunoblotting

GST pull-down assay was performed to analyze protein–protein interactions. To examine the interaction and inhibitory effect of morin, GST-bead-fused progerin (residues 566–606 and 657–664) was incubated with HEK293 cell extracts transfected with GFP-tagged lamin A (GFP-lamin A) and morin at room temperature for 1 h. After incubation, the samples were centrifuged at 3000*g* for 2 min, and the pellet (PPT) and supernatant (Sup) were divided. After washing the pellet with PBS, precipitates were collected and separated by sodium dodecyl sulphate–polyacrylamide gel electrophoresis (SDS-PAGE), and western blotting was performed using anti-GFP, actin, and GST. Actin was used as the negative control. Protein samples were extracted from cells with RIPA buffer (50 mM Tris-Cl, pH 7.5, 150 mM NaCl, 1% NP-40, 0.1% SDS, and 10% sodium deoxycholate). The samples were separated by SDS-PAGE and transferred to polyvinylidene fluoride membranes. Blotted membranes were blocked with 3% skim milk for 1 h and incubated with specific primary antibodies overnight at 4 °C. After washing with TBST, the membranes were reacted with HRP-conjugated secondary antibodies for 1 h. Finally, the membranes were washed with TBST and visualized using ECL solution and X-ray films. The following antibodies were used in this study: actin (sc-1616), GST (sc-138), GFP (sc-8036), and lamin A/C (sc-376248) from Santa Cruz Biotechnology (Santa Cruz, CA, USA). Progerin (ab66587) and H3K9me3 (ab8898) were purchased from Abcam (Cambridge, UK). HRP-conjugated goat anti-mouse, goat anti-rabbit, and mouse anti-goat antibodies (Pierce, Thermo Fisher Scientific, Inc., Rockford, IL, USA) were used as secondary antibodies.

4.9. Immunofluorescence staining

Cells were seeded on a cover glass and transfected with GFP-lamin A and GFP-progerin vectors. After 12 h of transfection, the cells were treated with morin or JH4 daily for 3 days. After fixation with 4% paraformaldehyde for 30 min at room temperature and permeabilization with 0.1% Triton X-100/PBS for 20 min, the cells were incubated with blocking buffer (PBS+ anti-human-Ab; 1:400) for 1 h. After washing with PBS twice, the cells were incubated with anti-lamin A/C, progerin, or H3K9me3 in blocking buffer (1:200) overnight at 4 °C. Finally, the cells were incubated with FITC or rhodamine-conjugated secondary antibodies in blocking buffer (1:400) at 4 °C for 6 h. The nucleus was stained with 4′,6-diamidino-2-phenylindole (DAPI) for 10 min. The cells were washed three times with PBS, and coverslips were mounted with mounting solution (H-5501; Vector Laboratories, Burlingame, CA, USA). Immunofluorescence signals were detected by fluorescence microscopy (Axioplan 2; Zeiss).

4.10. Quantification of cells with nuclear envelope deformation

Nuclear deformation was detected using the immunofluorescence images of lamin A/C or GFP-LA/PG. The abnormality of the nuclear membrane was determined based on nuclei (lamin A/C or GFP-LA/PG lining) containing blebs, invaginations, lobulations, and irregular contours. Depending on lamin A/C or GFP-LA/PG staining, the cells containing nuclear deformation were counted in randomly selected fields. Cell counting was performed in three independent experiments, and the experiments were conducted with three coverslips in one well.

4.11. RNA isolation and RT-PCR

For RT-PCR, total cellular RNA was extracted using an RNA extraction kit (Qiagen, Maryland, USA). After measuring the RNA concentration, 1 μg of total RNA was reverse-transcribed to cDNA using MMLV RT (Invitrogen) and random hexamers. RT-PCR was performed using the following specific primers: LMNA (5′-AAGGAGATGACCTGCTCCATC-3′ and 5′- TTTCTTTGGCTTCAAGCCCCC-3′), DcR2 (5′- ACTGGGAAAACCCCAGCAGCG-3′ and 5′- TTCCAGCAGACGCTGTGGCTC −3′), and GAPDH (5′-ATCTTCCAGGAGCGAGATCCC-3′ and 5′- AGTGAGCTTCCC GTTCAGCTC-3′).

Acknowledgments

This study was supported by grants from the National Research Foundation of Korea (2019R1A2C208513512). In addition, this study was supported by the Basic Research Program through the National Research Foundation of Korea (NRF) funded by the MSIT (2020R1A4A101932211).

Appendix A. Supplementary material

Supplementary data to this article can be found online at https://doi.org/10.1016/j.jff.2020.104331.

References

Ahn, J., Jo, I., Kang, S. M., Hong, S., Kim, S., Jeong, S., … Ha, N. C. (2019a). Structural basis for lamin assembly at the molecular level. *Nature Communications, 10*(1), 3757.
Ahn, J., Jo, I., Kang, S. M., Hong, S., Kim, S., Jeong, S., … Ha, N. C. (2019b). Structural basis for lamin assembly at the molecular level. *Nature Communications, 10*.
Alpers, D., Gallhof, M., Stark, C. B., & Brasholz, M. (2016). Photoassisted oxidation of ruthenium(II)-photocatalysts Ru(bpy)3(2+) and Ru(bpz)3(2+) to RuO4: Orthogonal tandem photoredox and oxidation catalysis. *Chemical Communications (Cambridge, England), 52*(5), 1025–1028.
Belaadi, N., Aureille, J., & Guilluy, C. (2016). Under pressure: Mechanical stress management in the nucleus. *Cells, 5*(2).
Booth-Gauthier, E. A., Du, V., Ghibaudo, M., Rape, A. D., Dahl, K. N., & Ladoux, B. (2013). Hutchinson-Gilford progeria syndrome alters nuclear shape and reduces cell motility in three dimensional model substrates. *Integrative Biology (Camb), 5*(3), 569–577.
Burke, B., & Stewart, C. L. (2002). Life at the edge: The nuclear envelope and human disease. *Nature Reviews Molecular Cell Biology, 3*(8), 575–585.
Butin-Israeli, V., Adam, S. A., Goldman, A. E., & Goldman, R. D. (2012). Nuclear lamin functions and disease. *Trends in Genetics, 28*(9), 464–471.
Cao, K., Blair, C. D., Faddah, D. A., Kieckhaefer, J. E., Olive, M., Erdos, M. R., … Collins, F. S. (2011). Progerin and telomere dysfunction collaborate to trigger cellular senescence in normal human fibroblasts. *Journal of Clinical Investigation, 121*(7), 2833–2844.
Cao, K., Capell, B. C., Erdos, M. R., Djabali, K., & Collins, F. S. (2007). A lamin A protein isoform overexpressed in Hutchinson-Gilford progeria syndrome interferes with mitosis in progeria and normal cells. *Proceedings of the National Academy of Sciences of the United States of America, 104*(12), 4949–4954.
Capell, B. C., & Collins, F. S. (2006). Human laminopathies: Nuclei gone genetically awry. *Nature Reviews Genetics, 7*(12), 940–952.
Chen, Z. Y., Chan, P. T., Ho, K. Y., Fung, K. P., & Wang, J. (1996). Antioxidant activity of natural flavonoids is governed by number and location of their aromatic hydroxyl groups. *Chemistry and Physics of Lipids, 79*(2), 157–163.
Cho, S., Irianto, J., & Discher, D. E. (2017). Mechanosensing by the nucleus: From pathways to scaling relationships. *Journal of Cell Biology, 216*(2), 305–315.
Chung, S. S., Oliva, B., Dwabe, S., & Vadgama, J. V. (2016). Combination treatment with flavonoid morin and telomerase inhibitor MST312 reduces cancer stem cell traits by targeting STAT3 and telomerase. *International Journal of Oncology, 49*(2), 487–498.
Collado, M., & Serrano, M. (2006). The power and the promise of oncogene-induced senescence markers. *Nature Reviews Cancer, 6*(6), 472–476.
De Sandre-Giovannoli, A., Bernard, R., Cau, P., Navarro, C., Amiel, J., Boccaccio, I., … Levy, N. (2003). Lamin a truncation in Hutchinson-Gilford progeria. *Science, 300*(5628), 2055.
Dechat, T., Pfleghaar, K., Sengupta, K., Shimi, T., Shumaker, D. K., Solimando, L., & Goldman, R. D. (2008). Nuclear lamins: Major factors in the structural organization and function of the nucleus and chromatin. *Genes & Development, 22*(7), 832–853.
Dechat, T., Shimi, T., Adam, S. A., Rusinol, A. E., Andres, D. A., Spielmann, H. P., … Goldman, R. D. (2007). Alterations in mitosis and cell cycle progression caused by a mutant lamin A known to accelerate human aging. *Proceedings of the National Academy of Sciences of the United States of America, 104*(12), 4955–4960.
Duenas, M., Gonzalez-Manzano, S., Gonzalez-Paramas, A., & Santos-Buelga, C. (2010). Antioxidant evaluation of O-methylated metabolites of catechin, epicatechin and quercetin. *Journal of Pharmaceutical and Biomedical Analysis, 51*(2), 443–449.
Fancy, D. A., Denison, C., Kim, K., Xie, Y. Q., Holdeman, T., Amini, F., & Kodadek, T. (2000). Scope, limitations and mechanistic aspects of the photo-induced cross-linking of proteins by water-soluble metal complexes. *Chemistry & Biology, 7*(9), 697–708.
Fong, L. G., Vickers, T. A., Farber, E. A., Choi, C., Yun, U. J., Hu, Y., … Young, S. G. (2009). Activating the synthesis of progerin, the mutant prelamin A in Hutchinson-Gilford progeria syndrome, with antisense oligonucleotides. *Human Molecular Genetics, 18*(13), 2462–2471.
Gadelha, I. C., Fonseca, N. B., Oloris, S. C., Melo, M. M., & Soto-Blanco, B. (2014). Gossypol toxicity from cottonseed products. *ScientificWorldJournal, 2014*, Article 231635.

Ghosh, S., & Zhou, Z. (2014). Genetics of aging, progeria and lamin disorders. *Current Opinion in Genetics & Development, 26*, 41–46.
Goldman, R. D., Shumaker, D. K., Erdos, M. R., Eriksson, M., Goldman, A. E., Gordon, L. B., … Collins, F. S. (2004). Accumulation of mutant lamin A causes progressive changes in nuclear architecture in Hutchinson-Gilford progeria syndrome. *Proceedings of the National Academy of Sciences of the United States of America, 101*(24), 8963–8968.
Gong, E. J., Park, H. R., Kim, M. E., Piao, S., Lee, E., Jo, D. G., … Lee, J. (2011). Morin attenuates tau hyperphosphorylation by inhibiting GSK3beta. *Neurobiology of Diseases, 44*(2), 223–230.
Hayflick, L. (1965). The limited in vitro lifetime of human diploid cell strains. *Experimental Cell Research, 37*, 614–636.
Hoffman, L. M., Smith, M. A., Jensen, C. C., Yoshigi, M., Blankman, E., Ullman, K. S., & Beckerle, M. C. (2020). Mechanical stress triggers nuclear remodeling and the formation of transmembrane actin nuclear lines with associated nuclear pore complexes. *Molecular Biology of the Cell, 31*(16), 1774–1787.
Hooper, C., Killick, R., & Lovestone, S. (2008). The GSK3 hypothesis of Alzheimer's disease. *Journal of Neurochemistry, 104*(6), 1433–1439.
Hur, E. M., & Zhou, F. Q. (2010). GSK3 signalling in neural development. *Nature Reviews Neuroscience, 11*(8), 539–551.
Khan, T., Abbasi, B. H., & Khan, M. A. (2018). The interplay between light, plant growth regulators and elicitors on growth and secondary metabolism in cell cultures of Fagonia indica. *Journal of Photochemistry and Photobiology B, 185*, 153–160.
Khan, T., Abbasi, B. H., Khan, M. A., Azeem, M. J. I. c., & products. (2017). Production of biomass and useful compounds through elicitation in adventitious root cultures of Fagonia indica. 108, 451–457.
Khan, T., Khan, T., Hano, C., Abbasi, B. H. J. I. C., & Products. (2019). Effects of chitosan and salicylic acid on the production of pharmacologically attractive secondary metabolites in callus cultures of Fagonia indica. 129, 525–535.
Kim, J. S., Piao, S., Lee, E., Yoon, B. Y., Moon, H. R., Lee, J., … Ha, N. C. (2013). Development of Akt-activated GSK3beta inhibitory peptide. *Biochemical and Biophysical Research Communications, 434*(4), 735–739.
Kim, K., Cha, J. S., Kim, J. S., Ahn, J., Ha, N. C., & Cho, H. S. (2018). Crystal structure of GSK3beta in complex with the flavonoid, morin. *Biochemical and Biophysical Research Communications, 504*(2), 519–524.
Lee, S. J., Jung, Y. S., Yoon, M. H., Kang, S. M., Oh, A. Y., Lee, J. H., … Park, B. J. (2016). Interruption of progerin-lamin A/C binding ameliorates Hutchinson-Gilford progeria syndrome phenotype. *Journal of Clinical Investigation, 126*(10), 3879–3893.
Lewandowska-Andralojc, A., & Polyansky, D. E. (2013). Mechanism of the quenching of the tris(bipyridine)ruthenium(II) emission by persulfate: Implications for photoinduced oxidation reactions. *Journal of Physical Chemistry A, 117*(40), 10311–10319.
Lilina, A. V., Chernyatina, A. A., Guzenko, D., & Strelkov, S. V. (2020). Lateral A11 type tetramerization in lamins. *Journal of Structural Biology, 209*(1), Article 107404.
McCord, R. P., Nazario-Toole, A., Zhang, H., Chines, P. S., Zhan, Y., Erdos, M. R., … Cao, K. (2013). Correlated alterations in genome organization, histone methylation, and DNA-lamin A/C interactions in Hutchinson-Gilford progeria syndrome. *Genome Research, 23*(2), 260–269.
Morris, Q., Gage, T., & Sh, W. (1951). The isolation and purification of morin on an ion-exchange resin. *Journal of the American Pharmaceutical Association, 73*, 3340–3341.
Nigg, E. A. (1992). Assembly and cell cycle dynamics of the nuclear lamina. *Seminars in Cell Biology, 3*(4), 245–253.
Piao, S., Lee, S. H., Kim, H., Yum, S., Stamos, J. L., Xu, Y., … Ha, N. C. (2008). Direct inhibition of GSK3beta by the phosphorylated cytoplasmic domain of LRP6 in Wnt/beta-catenin signaling. *PLoS ONE, 3*(12), Article e4046.
Pollex, R. L., & Hegele, R. A. (2004). Hutchinson-Gilford progeria syndrome. *Clinical Genetics, 66*(5), 375–381.
Rice-Evans, C. A., Miller, N. J., & Paganga, G. (1996). Structure-antioxidant activity relationships of flavonoids and phenolic acids. *Free Radical Biology and Medicine, 20*(7), 933–956.
Scaffidi, P., & Misteli, T. (2006). Lamin A-dependent nuclear defects in human aging. *Science, 312*(5776), 1059–1063.
Shumaker, D. K., Dechat, T., Kohlmaier, A., Adam, S. A., Bozovsky, M. R., Erdos, M. R., … Goldman, R. D. (2006). Mutant nuclear lamin A leads to progressive alterations of epigenetic control in premature aging. *Proceedings of the National Academy of Sciences of the United States of America, 103*(23), 8703–8708.
Ward, G. E., & Kirschner, M. W. (1990). Identification of cell cycle-regulated phosphorylation sites on nuclear lamin C. *Cell, 61*(4), 561–577.
Wu, T. W., Zeng, L. H., Wu, J., & Fung, K. P. (1994). Morin: A wood pigment that protects three types of human cells in the cardiovascular system against oxyradical damage. *Biochemical Pharmacology, 47*(6), 1099–1103.
Yang, S. H., Bergo, M. O., Toth, J. I., Qiao, X., Hu, Y., Sandoval, S., … Fong, L. G. (2005). Blocking protein farnesyltransferase improves nuclear blebbing in mouse fibroblasts with a targeted Hutchinson-Gilford progeria syndrome mutation. *Proceedings of the National Academy of Sciences of the United States of America, 102*(29), 10291–10296.
Yugarani, T., Tan, B. K., Teh, M., & Das, N. P. (1992). Effects of polyphenolic natural products on the lipid profiles of rats fed high fat diets. *Lipids, 27*(3), 181–186.
Zhang, Q., Zhang, F., Thakur, K., Wang, J., Wang, H., Hu, F., … Wei, Z. J. (2018). Molecular mechanism of anti-cancerous potential of Morin extracted from mulberry in Hela cells. *Food and Chemical Toxicology, 112*, 466–475.